Monte Carlo study of the pure and dilute Baxter–Wu model

Monte Carlo study of the pure and dilute Baxter–Wu model

Nir Schreiber and Joan Adler

Physics Department, Technion, Israel Institute of Technology, Haifa, Israel, 32000

Abstract
We studied the pure and dilute Baxter–Wu (BW) models using the Wang–Landau (WL) sampling method to calculate the density-of-states (DOS). We first used the exact result for the DOS of the Ising model to test our code. Then we calculated the DOS of the dilute Ising model to obtain a phase diagram, in good agreement with previous studies. We calculated the energy distribution, together with its first, second and fourth moments, to give the specific heat and the energy fourth order cumulant, better known as the Binder parameter, for the pure BW model. For small samples, the energy distribution displayed a doubly peaked shape, and finite size scaling analysis showed the expected reciprocal scaling of the positions of the peaks with L. The energy distribution yielded the expected BW $\alpha = 2/3$ critical exponent for the specific heat. The Binder parameter minimum appeared to scale with lattice size L with an exponent θ_B equal to the specific heat exponent. Its location (temperature) showed a large correction-to-scaling term $\theta_1 = 0.248 \pm 0.025$. For the dilute BW model we found a clear crossover to a single peak in the energy distribution even for small sizes and the expected $\alpha = 0$ was recovered.

PACS numbers: 05.10.Ln, 05.50.+q, 02.70.Rr

(Some figures in this article are in colour only in the electronic version)

1. Introduction

The two-dimensional Ising model has received such widespread attention as the paradigm system for phase transitions, that one sometimes says that a certain system is the 'Ising model' of a class of problems. While it is clearly special, it is not the only two-dimensional model of phase transitions with an exact expression for its free energy. Its critical behaviour is, in fact, rather atypical relative to many other two-dimensional systems and even to the three-dimensional Ising model, especially in the specific heat, where its critical exponent, α, is zero. The nature of the corrections-to-scaling in the spin $1/2$ Ising model is also very different to that of many other interesting systems.
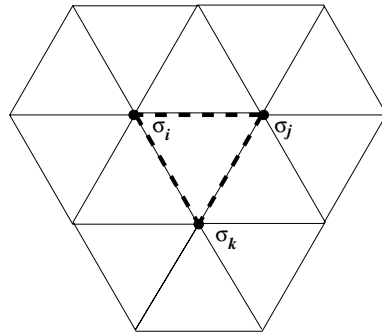
Figure 1. The energy of a given configuration is the sum of all interacting triangles formed by nearest neighbour spins.

Another spin system, now known as the Baxter–Wu (BW) model, was solved by Baxter and Wu [1, 2]. Spins $\sigma_i = \pm 1$, are situated on the triangular lattice and interact via a three spin interaction,

$$\mathcal{H} = -J \sum_{i,j,k} \sigma_i \sigma_j \sigma_k, \tag{1}$$

where i, j and k are the vertices of a triangle as shown in figure 1. $J > 0$ is the ferromagnetic coupling between nearest neighbour spins. The BW model exhibits a second order phase transition with its critical temperature (T_c) given by $2J/kT_c = \ln(1 + \sqrt{2}) = 2.269\,18\ldots$ (the same numerical value as for the Ising model on the square lattice). The specific heat critical exponent is equal to the correlation length exponent, $\alpha = \nu = 2/3$. Series-expansion results [3] gave the conjectured magnetization exponent of $\beta = 1/12$ and a susceptibility exponent of $\gamma \approx 1.17$ [4]. The latter confirmed the prediction of $\gamma = 7/6$ from the well-known scaling relation $\alpha + 2\beta + \gamma = 2$ [5, 6]. Real space renormalization group methods have also been used [7–9] to study the pure model, and the critical eigenvalues obtained gave critical exponents consistent with series-expansion and exact results. An exact form for BW corrections-to-scaling was found by Joyce [10] who conjectured that the spontaneous magnetization varied as $M = t^\beta (f_0(t) + t^{2/3} f_1(t) + \cdots)$ with analytic functions f_0, f_1 of the distance $t = (T - T_c)/T_c$. Adler and Stauffer confirmed this with series and metropolis Monte Carlo estimates [11].

Dilute Ising models are also somewhat famous, but for rather different reasons, as they have been the source of a great deal of controversy. Presumably because of the anomalous specific heat structure in the pure case, numerical work in the dilute regime, especially near the pure limit, is painful, and although a majority of authors (see, e.g., Roder *et al* [12]) have claimed that the controversy is resolved in favour of SSL theory [13–15], more study is useful.

The annealed dilute BW model was studied by Kinzel, Domany and Aharony [16] who showed from this exploration that its dominant critical behaviour is in the universality class of the four state Potts model, although the Potts model has logarithmic correction terms for this case. Domany and Riedel [17], argued the same for the pure BW model by means of symmetries of the Landau–Ginzburg–Wilson Hamiltonian. (Note that there are first order fixed points in the neighbourhood of these models). The quenched dilute BW model was studied by Landau and Novotny [18], who found a substantial change in the critical behaviour of the specific heat [19] for an impurity concentration of $1 - x = 0.1$. They also conjectured that the zero temperature threshold concentration above which no long-range order could be seen was about $x_c \simeq 0.71$. (See also results from a cluster-algorithm study of this system [20].)

More recent calculations [21, 22] showed that the value of x_c is even higher ($x_c \simeq 0.755$), and is bounded by $x_c^{\text{low}} = 0.710 \pm 0.001$ and $x_c^{\text{high}} = 0.784 \pm 0.004$. This is substantially above the value for Ising models where x_c is simply the percolation threshold of the corresponding lattice, which is rarely above 0.5.

Recently Wang and Landau [23, 24] proposed a very efficient algorithm for calculating the density-of-states (DOS) (i.e. the degeneracy of any level in energy space), $g(E)$, for Ising models and some related systems. To explore the issues of both pure and dilute BW models further, and to see how their different particulars of large α and corrections to scaling emerge from the calculation of the DOS, we have chosen to apply the WL algorithm to both the pure and quenched dilute BW models, and to study the behaviour of the energy distribution and related moments [25, 26] using the simulated DOS. The DOS of the pure and dilute Ising models was studied for comparison purposes.

In the next section we discuss the WL algorithm. In section 3 we present a comparison of an exact calculation of the DOS for the Ising model [27] with simulations using WL and give some results for the dilute Ising case. In section 4 we give in detail our results for the pure BW model, and in section 5 the results for the dilute BW model are presented. Finally we discuss the implications of our results in section 6.

2. The simulation method

Conventional Monte Carlo (MC) methods [28–30] generate the canonical energy distribution at a given temperature T_0. It is usually narrowly peaked around this temperature. The need to perform multiple simulations in order to obtain thermodynamics in a large range of temperatures requires a large computational effort. Other methods based on histogram accumulation [26, 31] approximate the distribution by the energy histogram at T_0. This distribution can then be reweighted to give statistics at another temperature. The reweighted distributions, however, are also restricted to a very narrow range of temperatures and suffer from large statistical errors in their tails for temperatures far from T_0. The broad histogram method [32] calculates the DOS through the consideration of the average number of visits to any two adjacent energy levels. Lee [33] offered the entropic sampling method using the observation that if the transition probability between any two energy levels is proportional to the ratio between the DOS of these levels, then a crude estimate to the DOS can be given when sampling at infinite temperature.

Wang and Landau improved Lee's method by introducing a modification factor which together with generating a 'flat' histogram (we have used the condition $|H(E) - \langle H \rangle|/\langle H \rangle \leqslant 0.05$ for any E), carefully controls the updating of the DOS. By dividing the energy space into different segments, and performing an independent random walk in each segment, one can generate very accurately, in a reasonable amount of CPU time, the DOS of the whole energy space, thus obtaining the canonical distribution at any desired temperature.

3. Ising model results

3.1. The pure Ising model

We began by validating the accuracy of our implementation of the WL algorithm against exact results for the Ising model on the square lattice with no impurities. A detailed comparison was made for the case of $L = 32$. The partition function for the Ising model on a lattice of
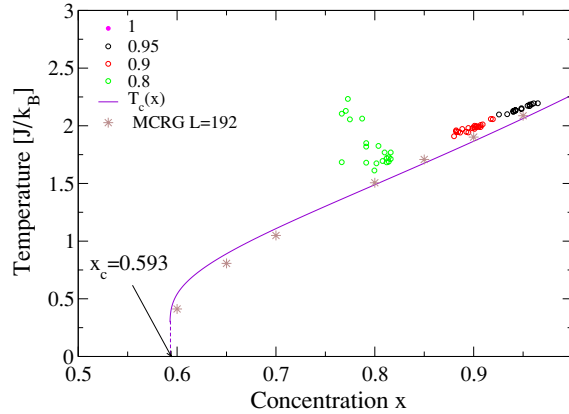
Figure 2. Critical line $T_c(x)$ in the T–x plane of the dilute Ising model. Small energy fluctuations for $x \leqslant 0.8$ make it hard to reliably determine $T_{C_{max}}$. The asterisks represent results from MC renormalization group calculations [37] and the solid line is the prediction $T_c(x) = \{\tanh^{-1}[e^{-1.45(x-x_c)}]\}^{-1}$, converging to the value of $x_c = p_c = 0.593$ [38].

length L can be written as a low temperature expansion

$$\mathcal{Z}_N = e^{2KN} \sum_\ell g_\ell x^{2\ell}, \tag{2}$$

where $N = L \times L$ is the number of spins, $K = J/kT$ is the reduced inverse temperature and $x = e^{-2K}$ is the low temperature variable. Each energy level can be labelled (relative to the ground state energy $-2JN$) by $E_\ell = 4J\ell$ ($\ell = 0, 2, 3, \ldots, N - 2, N$), so that g_ℓ is its corresponding DOS. Beale [27] used an extension of Onsager's solution [34] to give the exact expression for the partition function on a finite lattice [35], and extracted the DOS coefficients from expansion (2). When we plotted our results on top of Beale's expression for the case of $L = 32$ we saw no deviations between the exact and the simulated data within the resolution of the figure. The relative error between the exact and simulated data was also plotted and was found to be three orders of magnitude smaller than the calculated DOS and two orders of magnitude larger from the systematic error due to the choice of the final modification factor $f_{final} = 0.001$. This showed that the choice of this quite large f_{final} was sufficient, so that only a relatively small number of iterations was required for all the simulations performed throughout this work.

Further results from the pure Ising simulations will be introduced for comparison purposes in section 4.

3.2. The dilute Ising model

We continued the validation process by studying the dilute Ising model at a lattice size of $L = 22$. The Hamiltonian for the dilute Ising model may be written as

$$\mathcal{H} = -J \sum_{i,j} \epsilon_i \epsilon_j \sigma_i \sigma_j, \tag{3}$$

where the random disorder variables ϵ_i take the values 0 and 1, such that their configurational average is equal to a dilution of $0 < x < 1$. We considered the position of the specific heat maxima, $T_{C_{max}}$, for different nominal concentrations centred around the values $x = 0.8, 0.9$ and $x = 0.95$, as indicated in figure 2. It is clearly seen that for large concentrations ($x \geqslant 0.9$)
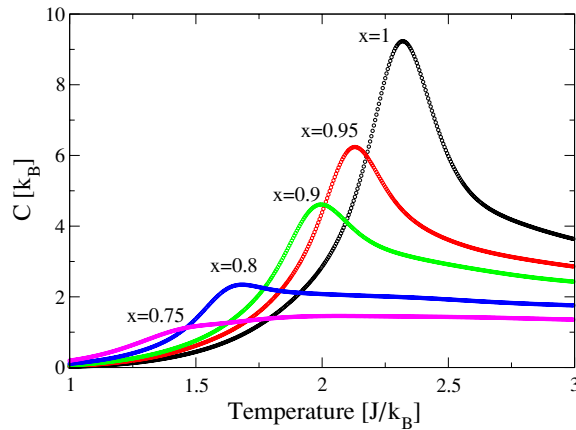
Figure 3. The specific heat of the dilute Ising model for different concentrations on a $L = 22$ lattice. For $x = 0.75$ there is no pronounced peak present.

the circles tend to a continuously critical line, slightly shifted from the solid line. The shift is a finite size effect due to the use of a small sample. For smaller concentrations there is a large dispersion of the circles and the data are less reliable. As shown in figure 3, the specific heat maximum becomes broader with decreasing concentration and is hard to locate precisely. The reason for this is that when lowering the concentration isolated clusters which rarely interact with each are formed, and hence energy fluctuations become smaller. For a concentration of $x = 0.75$ these fluctuations are also nearly constant and therefore no pronounced peak can be identified. It should be noted that presumably, when much larger samples would be used, a pronounced peak should be clearly seen for concentration even lower than $x = 0.75$ (see, for example, [36]). In the absence of analytic results, the location of our points close to earlier estimates validates both our dilute code and our analysis methods.

4. The pure Baxter–Wu model

We calculated the DOS for the BW model using lattice sizes L ranging from 6 to 120, with periodic boundary conditions being imposed. For each lattice size the data were collected separately for each energy segment and then were combined to give the density of states for the entire energy landscape. We averaged over nine different runs for $L = 30$, and saw that the fluctuations were three orders of magnitude smaller than the measured quantity ($\ln g$), so that we neglected these fluctuations and for each lattice size we executed a single run per segment only. By symmetry, for any state with negative energy, there exists a state with positive energy, so that it was sufficient to carry out the random walk only for non-positive energies. (A similar argument holds for the Ising model.) Plots of the internal energy, specific heat, free energy and entropy are given in figure 4.

Early simulations [18] showed the formation and motion of domains around the ferromagnetic and ferrimagnetic ground states, due to the special connectivity of the BW model, causing low frequency large energy fluctuations. These fluctuations made the impression that the system was in a metastable state, thus indicating a first order transition. In figure 5 we examined the energy distribution at $T_{C_{\max}}$ and found a doubly peaked curve (see [39]). The system appears to fluctuate between these two peaks denoted by E_-, corresponding to an 'ordered' state (more negative) energy, incorporating small clusters,
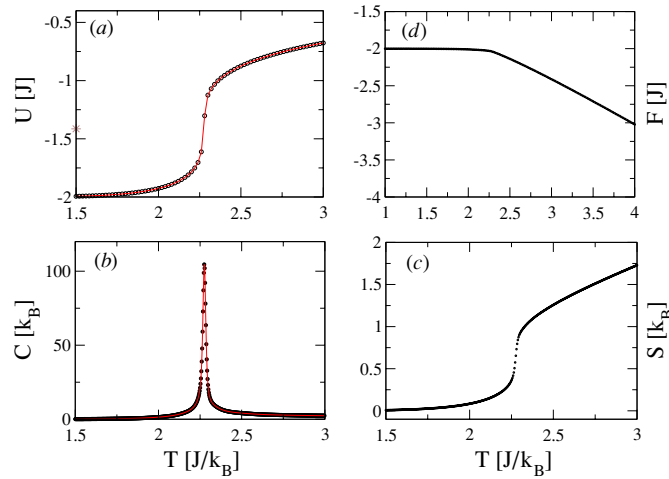
Figure 4. Calculation of thermodynamic functions for the pure BW model on an $L = 54$ lattice: (*a*) internal energy, (*b*) specific heat, (*c*) entropy and (*d*) free energy. The specific heat displays a very clear pronounced peak at the transition point.
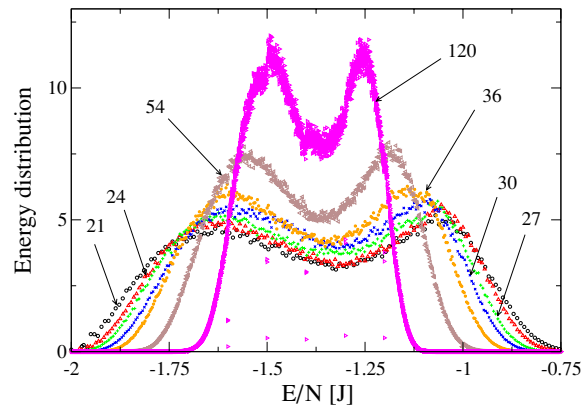

Figure 5. Critical distribution calculated at $T_{C_{max}}$ for the pure BW model. The lattice sizes are denoted by arrows. The $L = 120$ data suffers from the systematic errors resulting from the DOS calculations for large systems.

and E_+, corresponding to a 'disordered' state energy incorporating large clustering. A plot of the distribution for the Ising model both at $T_{C_{max}}^{Ising}$ and at $T_{C_{max}}^{BW}$ shows clearly sharp single peaks centred approximately at the critical energy $U_c = -\sqrt{2}J$ (figure 6). This supports the uniqueness of the distributions in figure 5. The positions (energies) of the peaks are found to scale with L^{-1} [39] as seen in figure 7, and are expected to eventually intersect for a large enough sample.

A comparison between the DOS of the Ising model and the BW model (figure 8) shows a significant difference between the two models. Although they have approximately the same number of different energy levels ($N - 1$ for Ising and $N - 3$ for BW), the function $\ln g$ appears to be concave everywhere in the interval $[-2, 0]$ for the Ising model, while for the BW graph this may not be so. This suggests an explanation for the appearance of the two peaks which is
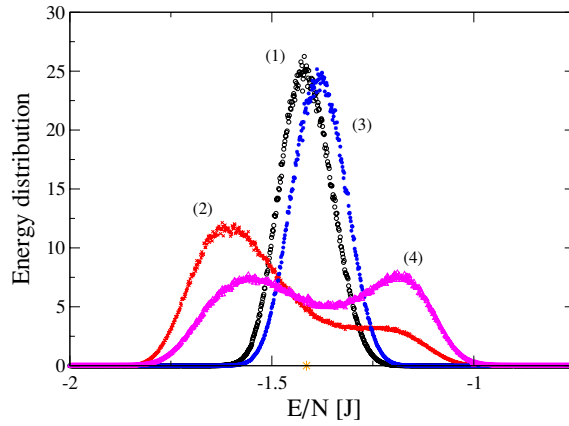
Figure 6. Energy distributions at $T_{C_{max}}^{Ising} = 2.28948 J/k_B$, at $T_{C_{max}}^{BW} = 2.27549 J/k_B$ and at the exact transition point T_c on the same lattice with $L = 54$. The numbers in parentheses denote: (1) Ising at $T_{C_{max}}^{BW}$, (2) BW at T_c, (3) Ising at $T_{C_{max}}^{Ising}$, (4) BW at $T_{C_{max}}^{BW}$. Note the distribution at the exact transition point (2) with the ratio of $r \simeq 4$ between the pronounced peak on the left and the 'hump' on the right [26]. The asterisk denotes their common critical energy $U_c = -\sqrt{2}J$.
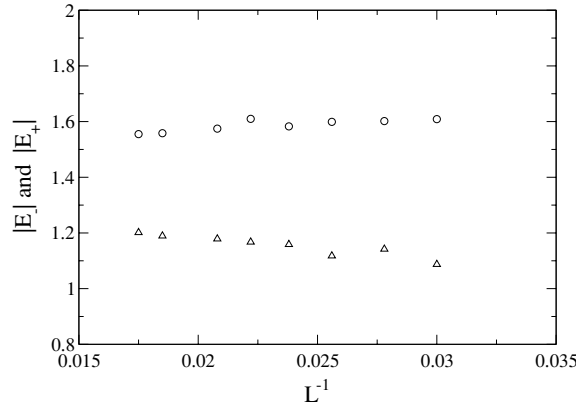
Figure 7. Variation of the energy distribution's two maxima positions with L^{-1}. The 'disordered' energies are denoted by ($\triangle$) and the 'ordered' energies by ($\circ$).

also consistent with the fact that they have the same height: the condition that the distribution will have *extrema* is satisfied by

$$d(\ln g)/dE = 1/kT. \tag{4}$$

If, at $T_{C_{max}}$, equation (4) has locally, a solution $f_1(E) = E/kT_{C_{max}} + C_1$ tangent to $\ln g$ at E_- and E_+, and another solution $f_1(E) = E/kT_{C_{max}} + C_2$ tangent to $\ln g$ at $U_c(L)$ (at the shifted critical energy, or the minimum between the peaks), then the distribution will have two peaks with equal height satisfying

$$p(E_-) = p(E_+) = e^{C_1}, \tag{5}$$

as seen in figure 5. This is essentially a finite size effect and should be recovered by a large enough sample, to give an 'Ising like' concave everywhere DOS function, and a single peaked distribution as its consequence.
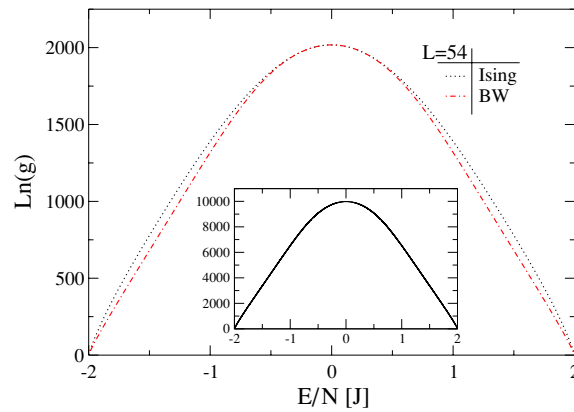
Figure 8. DOS of BW and Ising models on the $L = 54$ lattice. The function $\ln g$ appears to be concave 'everywhere' in $[-2, 0]$ for the Ising model, while this may not be so in the BW case. A plot of $\ln g(E)$ versus E for a larger BW system (120×120) is given in the inset.
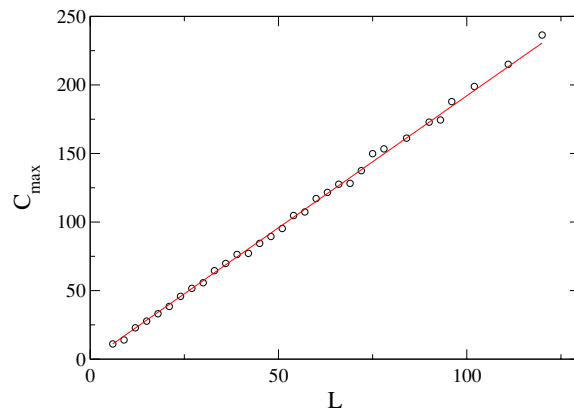

Figure 9. Scaling of the specific heat maxima with the length L for the pure BW model. The predicted $C_{\max}(L) \propto L$ behaviour is indicated by a solid line.

We further calculated the specific heat for each lattice size and then plotted its maximal value $C_{\max}$ versus L. We see in figure 9 a very nice agreement between the calculated data and the second order ansatz $C_{\max}(L) \propto L^{\alpha/\nu}$, with $\alpha/\nu = 1$, even for very small lattices ($L = 6$).

Another quantity of interest was the so-called Binder parameter [40, 41]

$$B = 1 - \frac{\langle E^4 \rangle}{3 \langle E^2 \rangle^2}, \tag{6}$$

where $\langle \cdots \rangle$ stands for the canonical thermal average. When we calculated the Binder parameter (whose plot as a function of temperature is given in figure 10), we saw a sharp inverse peak that usually occurs in first order transitions [25, 26]. Another manifestation of the strong finite size effects is the very precise (though quite unreliable) estimate of $T_c = 2.2696 \pm 0.0004$ to the transition point we obtained, when performing first order finite size scaling theory to the position of $B_{\min}$, $T_{B_{\min}}$.
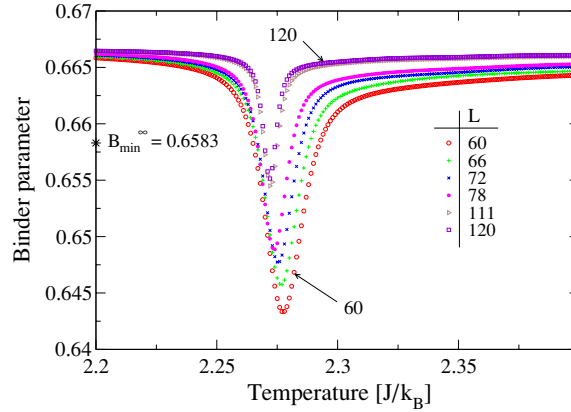
Figure 10. The Binder parameter for the pure BW model versus temperature, for various lattice sizes, from top ($L = 120$) to bottom ($L = 60$) in descending order. The Binder parameter is seen in the figure to display an inverse peak whose depth decreases as the system size increases. The infinite volume upper bound B_{min}^{∞} was estimated using first order scaling theory to $B_{min}(L)$.

Obviously, since the transition is continuous and therefore no ordered and disordered states coexist at the transition point, the critical probability distribution in the infinite volume limit is expected to be single peaked, causing B_{min} to eventually vanish with some exponent and the Binder parameter to take the trivial value of 2/3 also at the critical point. It was therefore convenient to repeat finite size scaling for B_{min} according to

$$B_{min} = \tfrac{2}{3} - \mathcal{B}_0 L^{-\theta_B/\nu}, \tag{7}$$

where θ_B is an exponent yet to be determined. In figure 13 we see the variation of the inverse distances $t_{C_{max}}^{-1} \equiv \left(T_{C_{max}} - T_c\right)^{-1}$ and $t_{B_{min}}^{-1} \equiv \left(T_{B_{min}} - T_c\right)^{-1}$, corresponding to the positions of the specific heat maxima and Binder parameter minima, respectively, with L. A least squares fit gave a slope of 1.529 ± 0.039 for the specific heat temperature and 1.748 ± 0.025 for the Binder parameter temperature. In accordance with [31]

$$T_{C_{max}} = T_c + A_0 L^{-1/\nu}(1 + A_1 L^{-\omega_1} + \cdots), \tag{8}$$

we use the analogy

$$T_{B_{min}} = T_c + B_0 L^{-1/\nu}(1 + B_1 L^{-\theta_1} + \cdots), \tag{9}$$

where ω_1 and θ_1 are correction exponents and A_0, A_1, B_0 and B_1 are amplitudes determined from simulations. It is therefore evident that $T_{B_{min}}$ displays a large correction-to-scaling term ($\theta_1 \simeq 0.25$), in contrast to the resulting $1/\nu$ scaling from the $T_{C_{max}}$ fit, which is in fair agreement with the exact 3/2 value, and which is also consistent with the scaling of C_{max}. It is also evident, however, from figure 14 and equation (7), that α and θ_B have the same value. Similar exact and simulational calculations of the Binder parameter for the Ising model on the same temperature scale (figure 11) showed much broader and less deep minima at $T_{B_{min}}$, suggesting that these minima vanish with an exponent θ_B larger than the BW exponent.

5. The dilute BW model

Let us consider now the ferromagnetic BW model with quenched impurities. The Hamiltonian is given by
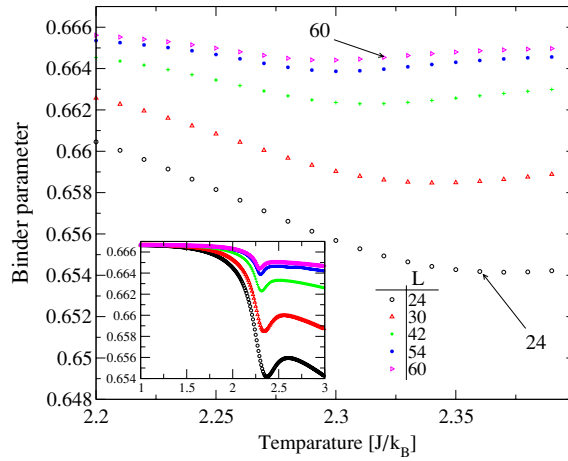
Figure 11. Temperature variation of the Binder parameter for the Ising model, from top ($L = 60$) to bottom ($L = 24$) in descending order. The data in the inset are given for the same lattices on a larger scale. The data for $L = 54$ are calculated using simulated DOS. All other data are exact.
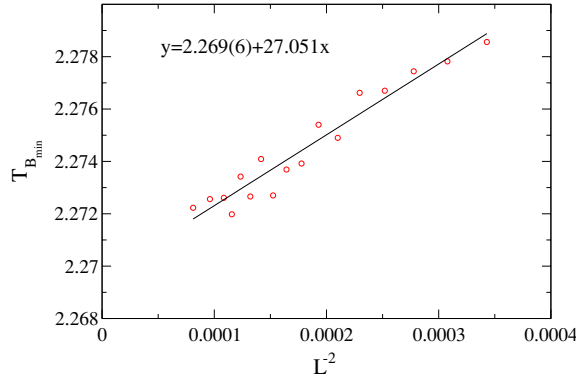

Figure 12. Scaling of $T_{B_{\min}}$ with the inverse volume of the system for the pure BW model.

$$\mathcal{H} = -J \sum_{i,j,k} \epsilon_i \epsilon_j \epsilon_k \sigma_i \sigma_j \sigma_k. \tag{10}$$

We studied systems with lengths L between 18 and 36. We kept concentrations of $x = 0.8$ for $L = 18$ and of $x = 0.9, 0.95$ and $x = 0.97$ for $L = 33$, fixed, and let them vary around $x = 0.9$ for $L = 33$. The data for $L = 24$ were calculated for concentrations varied around different values from $x = 0.85$ to $x = 0.97$. In figure 15 we compare the DOS of the pure and dilute BW models. The apparent crossover to a manifestly clear second order transition may give rise again to a concave 'everywhere' form of $\ln g$, already seen for the Ising model in figure 8. The energy levels differ now only in the amount of $2J$ and can take even or odd values for the same lattice size, depending on the vacancy distribution. We then performed a calculation similar to that made above for the dilute Ising model, of $T_{C_{\max}}$, to obtain the $T_c(x)$ critical line on a lattice with $L = 24$, and then fitted the high concentration data into a continuous (dotted) line (figure 16). All the data except for the $L = 18$ with a vacancy concentration of 0.2, which was, as for the dilute Ising model, unreliable because of relatively
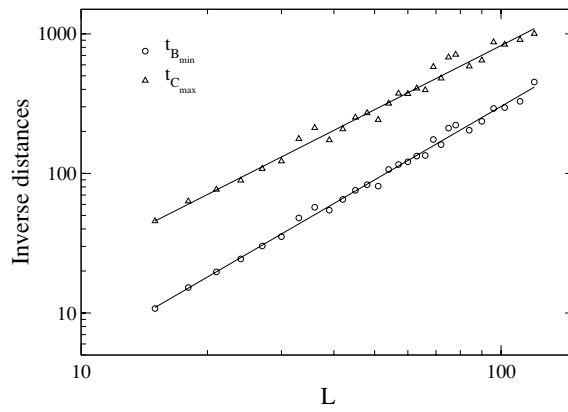
Figure 13. Scaling of the inverse distances $t_{C_{max}}^{-1}$ and $t_{B_{min}}^{-1}$, with L, for the BW model. The larger slope of the Binder parameter position's fit, may be a result of the large correction term θ_1 (see equation (9)). The specific heat data were shifted for ease of reading.
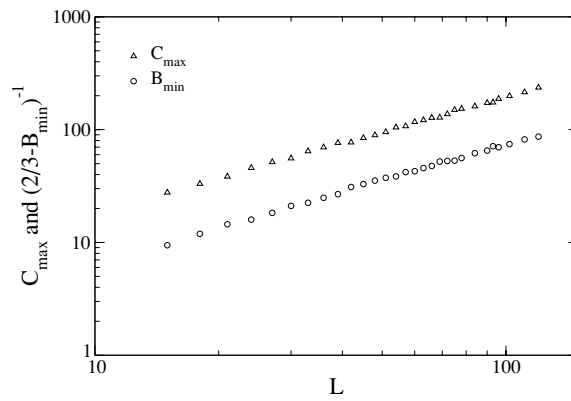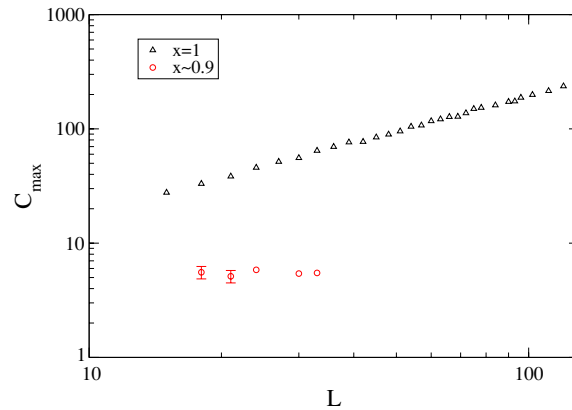

Figure 14. Scaling of the quantity $(2/3 - B_{min})^{-1}$ and the specific heat maximum C_{max}, with L, for the BW model.
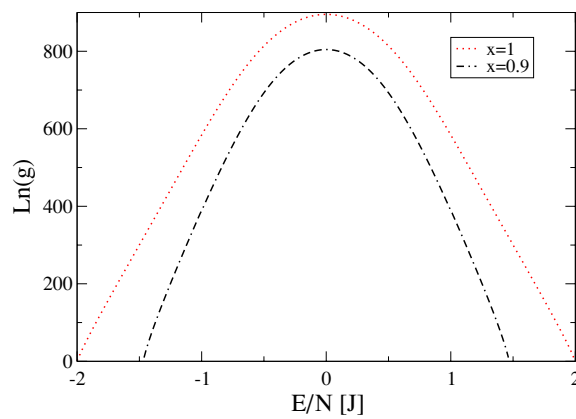
Figure 15. DOS for a pure (upper curve) and for a dilute (lower curve) BW model with $x = 0.9$, on an $L = 36$ lattice.
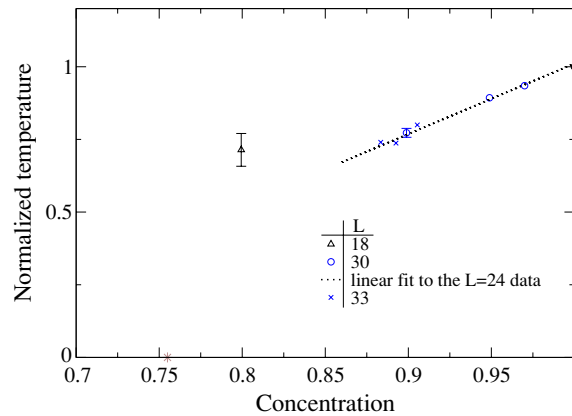
Figure 16. Normalized critical temperature for fixed concentrations on different lattice sizes for the dilute BW model.

Figure 17. Finite size scaling of C_{max} with L for the pure and dilute BW models. The data for the dilute model reveal an α exponent close to zero.

high dilution, fell very well on the dotted line. This may suggest that the critical behaviour is rather universal for large enough concentrations, because due to the special connectivity of the BW model, one would expect smaller energy fluctuations and therefore a larger scatter of data for large enough vacancy concentrations, whilst the dilute BW data seem to agree with the dilute Ising data for concentrations of $x \geqslant 0.9$. Of course, in order to make definitive statements about universality, larger samples would be needed than those used here.

We performed a rough finite size scaling for the specific heat maxima at a concentration of $x = 0.9$, using the three points measured for $L = 33$ that were averaged and the other data collected for fixed concentrations. Novotny and Landau [18] predicted $\alpha/\nu \simeq 0$ for a concentration of 0.9. Our results, presented in figure 17, also indicate, at least qualitatively, a significant change in α. Since spatial correlations become smaller and hence ν becomes smaller, the value of α substantially decreases, thus indicating an 'Ising like' singularity at the finite lattice transition point. Moreover, the Harris criterion for the diluted case is hereby confirmed. Another question of interest was the influence of vacancies on the nature of the transition. In order to make a statement regarding this question we plotted in figure 18
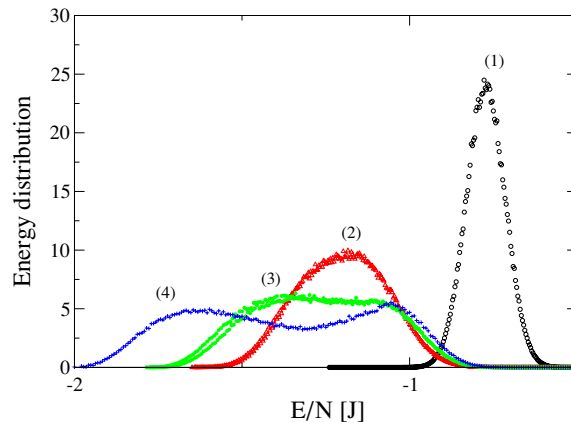
Figure 18. Critical energy distribution for various concentrations and critical temperatures, calculated on an $L = 24$ lattice. The numbers in parenthesis denote: (1) $x = 0.85$; $T_c = 1.749\,26$, (2) $x = 0.95$; $T_c = 1.933\,79$, (3) $x = 0.97$; $T_c = 2.076\,71$ and (4) $x = 1$ (pure); $T_c = 2.291\,64$. The distribution is seen to become sharper and narrower when the concentration is reduced.

the energy distribution for different concentrations. We see clearly and unsurprisingly that lowering the concentration causes the doubly peaked distribution to vanish and become a singled peaked one with a narrower width centred away from U_c. It may then be plausible to say that in contrast to energy fluctuations which become negligible at sufficiently low concentrations, magnetic fluctuations increase with increasing dilution and the transition is manifestly second order.

6. Conclusions

Our simulations have shown that the WL sampling is a very accurate algorithm. The thermodynamic quantities resulting from the calculated $g(E)$, which yield reasonable quality critical data, provide good evidence for this.

Our results show that the pure Baxter–Wu model is strongly influenced by finite size effects and corrections to scaling. The scaling of the specific heat maxima is in excellent agreement with the second order form $C_{\max} \propto L^{\alpha/\nu}$, even for small lattices, and no correction terms are observed. The Binder parameter, however, displays large minima for small samples, thus incorrectly could be thought of as a 'first order' scaling field. It is an 'irrelevant' field in the sense that it gives no additional information about the universal exponent ν, but rather vanishes with an exponent θ_B. This exponent is also evident in the Ising model and is presumably larger for this model. The vanishing inverse peak in both models states that the energy distribution approaches a delta function in the thermodynamic limit, although it is essentially non-Gaussian. The doubly peaked shape of the latter is rather peculiar. One would usually expect a single peaked distribution which becomes narrower, the closer to criticality one is. This shape is essentially a finite size effect due to the large fluctuations between the ferromagnetic and ferrimagnetic clusters formed in the vicinity of the transition point, and will eventually vanish in the thermodynamic limit. The WL method is also very successful when applied for the dilute BW model even for small lattices, both in terms of the critical isotherm in temperature-concentration plane for a weak dilution, and probability distribution. A crossover to a single peaked critical distribution is clearly seen when decreasing the concentration of

spins, and a single peaked distribution is evident at a concentration of $x = 0.85$. This is a result of the formation of isolated domains causing relatively small energy fluctuations around the critical energy.

It would be interesting in the future to use larger lattices to confirm our explanations of the finite size problems. The relatively high accuracy of the WL method for small dilute systems could be applied in the future to study disorder in other models.

Acknowledgments

References

[1] Baxter R J and Wu F Y 1973 *Phys. Rev. Lett.* **31** 1294
[2] Baxter R J and Wu F Y 1974 *Aust. J. Phys.* **27** 357
[3] Watts M G 1974 *J. Phys. A: Math. Nucl. Gen.* **7** L85
     Sykes M F and Watts M G 1975 *J. Phys. A: Math. Gen.* **8** 1469
     Baxter R J, Sykes M F and Watts M G 1975 *J. Phys. A: Math. Gen.* **8** 245
[4] Griffiths H P and Wood D W 1973 *J. Phys. C: Solid State Phys.* **6** 2533
     Wood D W and Griffiths H P 1974 *J. Phys. C: Solid State Phys.* **7** 1417
[5] Essam J W and Fisher M E 1963 *J. Chem. Phys.* **38** 802
[6] Rushbrooke G S 1963 *J. Chem. Phys.* **39** 842
[7] Braathen H J and Hemmer P C 1975 *Phys. Nor.* **8** 69
[8] Imbro D and Hemmer P C 1976 *Phys. Lett.* A **57** 297
[9] den Nijs M P M, Pruisken A M M and Van Leeuwen J M J 1976 *Physica* A **84** 539
[10] Joyce G S 1975 *Proc. R. Soc. Lond.* A **345** 277
[11] Adler J and Stauffer D 1992 *Physica* A **181** 396
[12] Roder A, Adler J and Janke W 1998 *Phys. Rev. Lett.* **80** 4697
[13] Shalaev B N 1984 *Sov. Phys. Solid State* **26** 1811
[14] Shankar R 1987 *Phys. Rev. Lett.* **58** 2466
[15] Ludwig A W W 1988 *Phys. Rev. Lett.* **61** 2388
[16] Kinzel W, Domany E and Aharony A 1981 *J. Phys. A: Math. Gen.* **14** L417
[17] Domany E and Riedel E K 1978 *J. Appl. Phys.* **49** 1315
[18] Novotny M A and Landau D P 1981 *Phys. Rev.* B **24** 1468
[19] Harris A B 1974 *J. Phys. C: Solid State Phys.* **7** 1671
[20] Novotny M A and Evertz H G 1993 *Computer Simulations in Condensed Matter Physics* vol 6 *(Springer Proceedings in Physics* vol 76*)* (Heidelberg: Springer) p 188
[21] Fried H 1992 *J. Phys. A: Math. Gen.* **25** 2545
[22] Adler J 1992 *Physica* A **177** 45
[23] Wang F and Landau D P 2001 *Phys. Rev. Lett.* **86** 2050
[24] Wang F and Landau D P 2001 *Phys. Rev.* B **64** 056101
[25] Challa Murty S S, Landau D P and Binder K 1986 *Phys. Rev.* B **34** 1841
[26] Janke W 1993 *Phys. Rev.* B **47** 14757
[27] Beale P D 1996 *Phys. Rev. Lett.* **76** 78
[28] Metropolis N, Rosenbluth A W, Rosenbluth M N, Teller A M and Teller E 1953 *J. Chem. Phys.* **21** 1087
[29] Swendsen R H and Wang J S 1987 *Phys. Rev. Lett.* **58** 86
[30] Wolff U 1989 *Phys. Rev. Lett.* **62** 361
[31] Ferrenberg A M and Landau D P 1991 *Phys. Rev.* B **44** 5081
[32] de Oliveira P M C, Penna T J P and Hermann H J 1998 *Eur. Phys. J.* B **1** 205
[33] Lee J 1992 *Phys. Rev. Lett.* **68** 9
[34] Onsager L 1944 *Phys. Rev.* **65** 117

[35] Kaufman B 1949 *Phys. Rev.* **76** 1232
[36] Selke W, Shchur L N and Vasilyev O A 1998 *Physica* A **259** 338
[37] de Souza A J F and Moreira F G 1992 *Europhys. Lett.* **17** 491
[38] Stauffer D and Aharony A 1994 *Introduction to Percolation Theory* (London: Taylor and Francis)
[39] Lee J and Kosterlirz J M 1992 *Phys. Rev. Lett.* **65** 137
[40] Binder K 1981 *Phys. Rev. Lett.* **47** 693
[41] Binder K 1981 *Z. Phys.* B **43** 119